Article

Interference Recommendation for the Pump Sizing Process in Progressive Cavity Pumps

Leandro Starke [1]*, Aurélio Faustino Hoppe [1] , Andreza Sartori [1] , and Valderi Reis Quietinho Leithardt [2,3]

1   Department of Information Systems and Computing, Regional University of Blumenau. Rua Antônio da Veiga 140, 89030-903 Blumenau, Brazil; (email: aureliof@furb.br; asartori@furb.br)
2   COPELABS, Lusófona University of Humanities and Technologies. Campo Grande 376, 1749-024 Lisboa, Portugal; (email: valderi@ipportalegre.pt)
3   VALORIZA, Research Center for Endogenous Resources Valorization. Instituto Politécnico de Portalegre, 7300-555 Portalegre, Portugal
*   Correspondence: leandro.starke@gmail.com

Abstract: Pump Sizing is the process of dimensional matching an impeller and stator to provide a satisfactory performance test result and good service life during the operation of progressive cavity pumps. In this process, historical data analysis and dimensional monitoring are done manually, consuming a large amount of man-hours and requiring a deep knowledge of progressive cavity pump behavior. This work presents the use of complex networks in the construction of a prototype to recommend interference during the Pump Sizing process in a Progressive Cavity Pump. For this, data from different expert applications were used in addition to individual control Excel spreadsheets to build the database used in the prototype. From the pre-processed data, complex network techniques and the Betweenness Centrality metric were used to calculate the degree of importance of each order confirmation, as well as to calculate the dimensionality of the rotors. The model was evaluated using the mean squared error (MSE), obtaining a MSE of 0.28 for the cases where there were recommendations for order confirmations. Based on the results obtained, it was realized that there is a similarity with the dimensional defined by design engineers during the Pump Sizing process.

Keywords: Rotor Dimensions; Complex Networks; Crossing Centrality; Rotor; Pump Sizing; Progressive Cavity Pump

---

1. Introduction

In 1933, the French mathematician and researcher René Moineau idealized the principle of progressive cavities. However, not having financial resources to develop his project, Moineau sold his patents to some companies. His principles resulted in the Progressive Cavity Pumping (PCP) lifting system, which is nowadays the main technology for oil well production in the world [1].

The BCP artificial lift method consists of a progressive cavity pump installed inside the well at the lower end of the production column through which fluid is pumped [1]. In Figure 1 (left), it can be seen that the progressive cavity pump basically consists of two components, a stator and an impeller, and is driven by the rotation of the impeller through the rod column. In addition, it can be noted in Figure 1 (right) the dimensions that are called major diameter (D) and minor diameter (d), both in the rotor and in the stator.
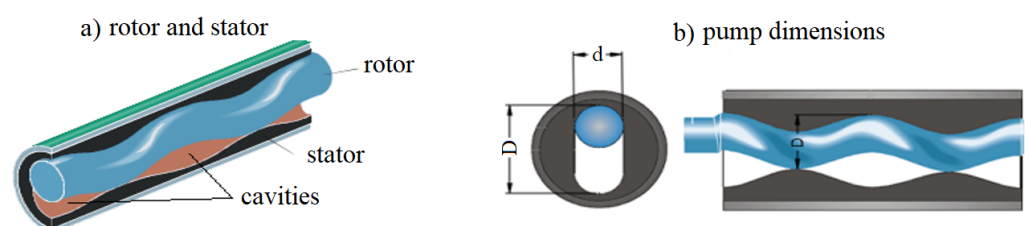

Figure 1. Rotor and stator with their dimensions: a) Rotor and stator; b) Pump dimensions.

There are several works focused on designing electrical machines with better efficiency and development of fault diagnostics [2], with applications optimizing the machine design through the finite element method (FEM) [3] and artificial intelligence [4]. Increasingly, FEM-based approaches are being successfully applied for the development of equipment that is more robust [5–7]. Even simple solutions can be used to improve the performance of electric motors by simply changing the way they are used [8]. On the other hand, artificial intelligence methods are being improved to obtain models with greater capacity. In this context, fault diagnosis can be performed by means of time series analysis [9–11], computer vision [12,13], pattern recognition [14–16].

During the rotation movement of the rotor, voids are formed and sealed in the cavity (Figure 1) of the stator, which are filled by the fluid to be pumped. With the rotation of the rotor, these voids move continuously and progressively in the direction of the helicoid pitch, dragging the fluid in the direction of the pump discharge. It is noteworthy that the ability to generate pressure difference of the BCP is controlled by a combination between the maximum pressure of each cavity and the number of cavities. How much pressure difference each cavity can generate is related to the ability to create seal lines between the rotor and stator and the properties of the pumped fluid. This seal line is improved according to the interference between rotor and stator, that is, the smaller the space created between them [17].

The creation of the seal line between the rotor and the stator happens by combining their dimensions (D and d), with this it is possible to obtain greater success in the result of the performance test on the bench, ensuring a good useful life of the pump in the well. This combination is called Pump Sizing. The lifetime of a BCP pump is determined by the interaction between rotor and stator in the sealing lines (interference) that are controlled by the pump sizing. The Pump Sizing process is very complex and requires rigorous studies on pump behavior on test benches, fluid composition, characteristics of the well where the pump will operate, among others. To simplify this process, many BCP pump manufacturers usually manufacture rotors with different dimensional ranges in the smallest diameter (d) and largest diameter (D) of the rotor for each pump model. These ranges are categorized as standard, single, double oversized or undersized [18].

Based on the arguments exposed above, this work presents the construction of a prototype that performs the interference recommendation and, as a result, calculates the rotor size so that it, combined with the stator can achieve the acceptance criteria obtained during the bench performance test. In addition, it is intended to simplify all the steps performed during Pump Sizing by increasing the number of examples that can be used as reference, resulting in a more assertive definition.

2. Proposed Method

This paper was organized according to the steps of the CRISP-DM model, starting with the phase of understanding the problem and its data, the selection and treatment of data until a solid and reliable database is achieved, the definition of possible techniques to be used in the construction of the interference recommendation, and finally the evaluation of the results.

In the stages of Business Understanding and Data Understanding, we followed up with the engineers who design Progressive Cavity Pumps that perform the Pump Sizing process. In this step, maximum understanding of the process and why it is important during the manufacturing of Progressive Cavity Pumps was obtained. In addition, all the tasks that are performed during the process were documented. Table 1 shows the 8 main tasks that are performed with each new input.

During the process documentation stage, the variables that directly and indirectly influence the test results of Progressive Cavity Pumps and relevant to Pump Sizing were also catalogued. With this, a total of 38 variables were obtained, among them are variables such as the pump model, test results, test criteria performed, and the complete dimensionality of the rotor and stator assembly that are directly linked to the test results obtained.

Table 1. Description of tasks performed in the Pump Sizing process.

No.	Task
01	Collect data of inlet pump test conditions
02	Search for similar pumps in the database
03	Search for the rotor and stator dimensions of similar pumps
04	Analysis of the rotor and stator dimensions of similar pumps
05	Interference calculation
06	Search for the current stator dimensions of the stator of the same pump model
07	Analysis of the stator dimensions of the pump model
08	Calculation of the rotor dimensions using the interferences

Currently, most of the variables are available in expert systems (non-integrated) with their own database, and another part are in Excel spreadsheets used by the design engineers. Given this scenario, it was decided as a starting point to select data from the system that stores all performance tests of Progressive Cavity Pumps, called Performance Curves. In this selection the pump serial number, order confirmation number, rotor code, test date, stator surface temperature, test fluid temperature and stator part code from the year 2019 were considered resulting in 8714 test records.

The data obtained from this selection went through the cleaning process, as they presented a large amount of typing errors and lack of specific fields within the system. In addition, data related to the stators underwent a transformation in its original structure, because stators can be built from one or more welded parts. In this case, the information stored for each complete stator had to be replicated, where each line represents a stator part that makes up the complete stator.

Once the data had been cleaned and processed, it was used to make a new selection, adding data regarding the test conditions of each order confirmation that are stored in the ERP [19]. In this selection, information was added to the data, such as the fluid used in the test, the rotation and pressure by which the test results will be evaluated for the pump acceptance, and the minimum and maximum limits of volumetric efficiency defined by the customer, which the pump must have to obtain acceptance. Finally, a dataset with 48,276 records and 37 columns was obtained, representing the entire path from the conception of the sales order for the pump to the final test on the test bench.

To use an approach similar to the process done manually, in which historical data is used to perform Pump Sizing, we chose to use complex networks to evaluate the influence that an Order Acknowledgment has in relation to the others. In modeling the network, we chose to consider it non-directed, because both vertices connected by edges are considered similar, and both can be used as reference to each other. Figure 2 shows a sample network in which each vertex represents an Order Acknowledgment and each edge represents one or more reference(s) to other Order Acknowledgments.
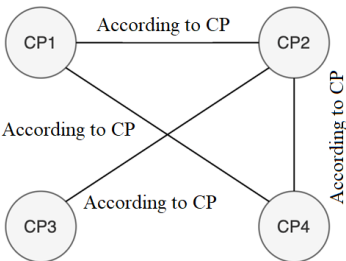

Figure 2. Network representation.

With the network modeled, we applied the algorithms for identifying connected components and calculating the Betweenness Centrality metric. A graph G (Figure 3a) is connected if there is a path connecting each pair of vertices of G, otherwise G is said to be disconnected. Thus, a disconnected graph has at least two connected subgraphs, called

connected components (Figure 3b). The graph neural networks (GNNs) are being most widely used for their ability to extract additional information from the data [20], in addition to GNNs, deep learning-based models are constantly being explored for their ability to learn nonlinear patterns [21–23]. Models that use ensemble aggregating weaker learners also have their place within this context [24–26].
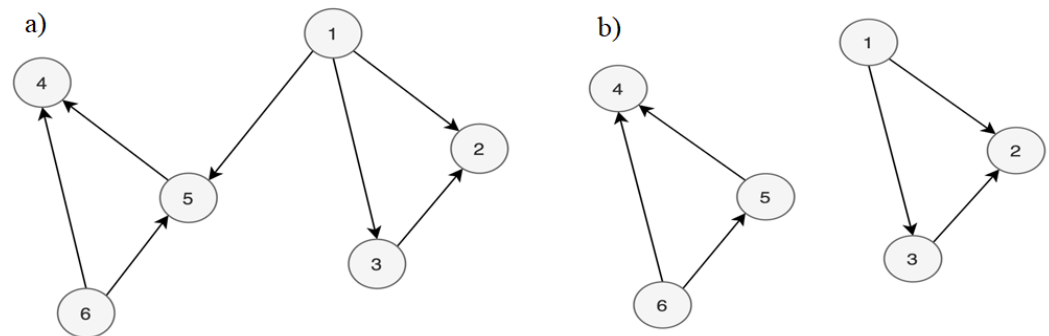

Figure 3. Graph: a) Connected components; b) Disconnected components.

Several frameworks have been used to solve graph-based problems, such as graph attention networks [27], graph convolutional networks [28], heterogeneous graph neural network [29], heterogeneous graph attention network [30], and so on. As well as classic neural network models [31–33] or models based on deep learning [34–36], the choice of the appropriate framework is critical for successful application.

The search for connected components returns a SET Generator with the Order Acknowledgments of the connected component. Identifying the connected components in this context is important for clustering Order Acknowledgments that were used as reference to perform Pump Sizing. Also, consequently, these connected components have a similarity in their technical characteristics, test criteria and test results in their Order Acknowledgments and can bring additional information to the analysis. In Figure 4 you can see the plot of 10 connected components of the network. Each color represents a connected component, where the vertices, the Order Acknowledgments.
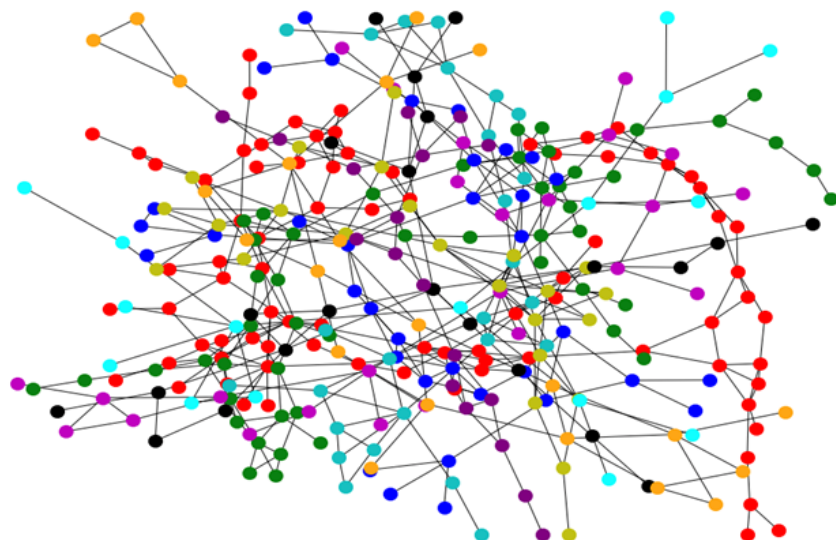

Figure 4. Connected components.

In scenarios that involve the use of GNNs, many make use of devices and communications that involve protocols. These applications can be extended to classification [37], and forecasting [38,39]. The graph approach could be extended to applications in health applications [40], entrepreneurship [41], telecommunications [42,43], power systems [44,45],

sustainability [46], industry applications [47,48], education [49], electric vehicles [50], internet of things [51–53], and fault identification in general [54,55]. Those are areas that are being developed and could have better evaluation results when GNNs are used.

With the related components defined, the Betweenness Centrality metric was calculated, determined by Equation 1.

$$cv(v) = \sum_{s,t \in V} \frac{\sigma(s,t|v)}{\sigma(s,t)} \tag{1}$$

where V is the set of vertices of the graph, $\sigma(s,t)$ is the number of minimal paths between vertices (s,t), and $\sigma(s,t|v)$ is the number of these minimal paths that pass through some vertex v other than (s,t), if $s = t, \sigma(s,t|) = 1$ and if $v \in s, t, \sigma(s,t||v) = 0$.

This metric is used to measure which Order Acknowledgment has the most influence on the connected component it is part of. The highest values of this metric are used as a recommendation and its data is used for Pump Sizing. The return is a dictionary where the key identifies the Order Acknowledgment number and the value is the return of Equation 1. In Table 2 you can see this dictionary.

Table 2. Return of the Betweenness Centrality metric.

{ 'B30000714': 0.0,
'B30000751': 0.0,
'N30000488': 0.0,
'N30000499': 0.0,
'N30000506': 14.0,
'N30000512': 27.0,
'N30000515': 67.0,
'N30000524': 47.0,
'N30000527': 0.0,
'N30000533': 0.0,
'N30000541': 27.0,
'N30000566': 0.0,
'P30002318': 0.0,
'P30002569': 0.0,
'P30002579': 71.0,
'P30002593': 0.0}

At the end of this process, you have a list of dictionaries where each dictionary is a connected component containing the Order Acknowledgment number as a key and the Betweenness Centrality value. A sample of the result of this step is shown in Table 3.

Table 3. List of related components with the Betweenness Centrality metric.

[{'L30006281': 0.0, 'L30006714': 0.0, 'L30006821': 2.0, 'L30006899': 0.0},
{'L30005944': 2.0, 'L30005947': 0.0, 'L30006162': 2.0, 'L30006163': 0.0},
{'L30005538': 0.0, 'L30005782': 0.0, 'L30006208': 3.0, 'L30006342': 0.0},
{'L30006566': 0.5, 'L30006622': 0.5, 'L30006656': 0.5, 'L30006669': 0.5},
{'P30002330': 0.0, 'P30002363': 2.0, 'P30002452': 0.0, 'P30002489': 0.0},
{'L30006628': 0.0, 'L30006693': 0.0, 'L30006789': 2.0, 'L30006890': 0.0}]

With the related components defined and each Order Acknowledgment having its Betweenness Centrality calculated, the step that performs the interference recommendation for the incoming Order Acknowledgment begins. Figure 5 shows the main actions performed to make the interference recommendation.
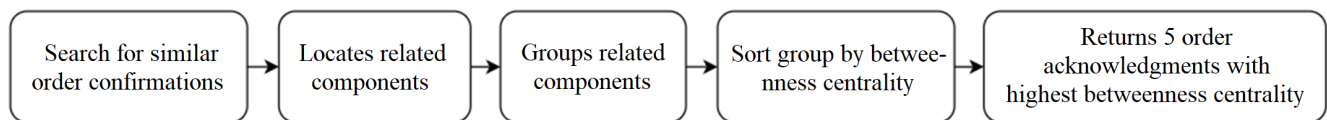
Search for similar order confirmations	→	Locates related components	→	Groups related components	→	Sort group by betwee-nness centrality	→	Returns 5 order acknowledgments with highest betweenness centrality

Figure 5. Steps for interference recommendation.

Initially, a search for Order Confirmations is applied to the data set considering the pump model, stator rubber and pump test parameters, then the related components to which each Order Confirmation is part are located, such connected components are grouped and ordered by the value of the Betweenness Centrality metric. With this, we have an ordered group of connected components that have similarity with the input. From this, the first 5 Order Confirmations with the highest value of Betweenness Centrality, that is, with the greatest influence, are selected.

Based on the five recommended Order Confirmations, their clashes are used to define the new clash. We chose to use the median central tendency measure for this definition, because it is known that there may still be outliers between the recommended cases and they can negatively influence the value of the new interference when the average is used.

To calculate the rotor dimensions, measurements "D" and "d" of the stator are necessary. In the current process, the stator dimensions are monitored to ensure that the dimensions are close to the stator dimensions of the recommended cases. This monitoring is necessary because changes in the process, changes in the rubber formulation, among others, can cause changes in the stator dimensional. This monitoring is extremely necessary otherwise the recommended interference will not be reached. It is noteworthy that the dimensions of the last thirty stators manufactured were used, calculating the average of the "d" of these cases. To search for these stators, parts of the data that make up the pump model and the type of stator rubber were used. The pump pressure was disregarded because it is not a variable that influences the stator dimensional change.

Finally, the rotor dimensions are calculated, applying the stator dimension found and the recommended interference. It is worth mentioning that, in order to calculate the rotor measurements, the most relevant dimensions and the ones that most influence the result of the bench test for each type of geometry were considered. Single-lobe pumps were calculated only the rotor measure "d" as shown in Equation 2 where, *de* is the smallest diameter of the stator and *i* the interference.

$$dr = de + i. \tag{2}$$

For Multi-lobe geometries Equation 3 was used. where, *dme* is the mean stator diameter and *i* is the interference.

$$dr = dme + i. \tag{3}$$

In addition, to calculate the dimensionality of the rotor with Multi-lobe geometry, it is necessary to calculate the mean stator diameter (*dme*), as shown in Equation 4.

$$dme = \frac{(De + de)}{2}. \tag{4}$$

3. Results Analysis

To test the proposed model, the data set with 48,276 records and 37 columns, resulting from the data selection and cleaning steps, was used. From these data, only the tests where the acceptance rotation was equal to the test rotation were considered, because the pump is tested in several rotations, in this case, only the data of the rotation of interest to which the pump will be evaluated is desired. Therefore, there was a reduction in the data set to 11,673 records.

These data, in turn, were divided into two parts, a part called training, with 80% of the records, which was used to build the network, and the second part called test, with 30% of the records, which were used as input for the recommendation. With the network constructed from the training data, the tests for the recommendation can be performed using the test data as input. In this step variables described in Table 1 categorized as input were considered. To evaluate the recommendations, it was decided to compare the average dimension "d" of the impeller in pumps with single-lobe geometry or the average dimension "d" of the impeller in pumps with multi-lobe geometry with their respective real average dimension. In Table 4 there is a sample of the input variables as well as the target variable y_true which is the real rotor dimensional and which will be compared with the recommended rotor dimensional y_rec defined by the recommendation.

Table 4. Input data and target variable.

Variable	Value	Type
type_tube	NTZ	Input
nominal_pipe_diameter	400.0	Input
pump_geometry	ST	Input
pump_flow	62.0	Input
high_pressure	YES	Input
rubber_stator	286.0	Input
test_fluid	0.0	input
temp_fluid_test	50.0	Input
temp_up_stator_test	30.0	Input
rpm_acceptance	300.0	Input
rpm_test	300.0	Input
pressure_acceptance	180.0	Input
efficiency_min	0.0	Input
eff_max	0.0	Input
y_true	41.48	Target
y_rec	41.26	Recommendation

A total of 2,972 tests were performed involving different pump models and test criteria. The first evaluation made on the recommendation was to quantify the number of cases in which it was successful in making recommendations. Within the 2,972 tests, 69% of the cases had recommendations, this happens because the recommendation did not find any Order Confirmation similar to the given inputs.

Next, the quality of the recommendation was checked, for this, the Mean Squared Error (MSE) metric was used, which calculates the difference between the real rotor measure and the recommended rotor measure, high MSE values, indicate that the recommendation did not perform well in relation to the recommendations. Applying this metric to the recommended data obtained a score of 0.28. It is worth noting that, to calculate the MSE metric, the cases in which there were no recommendations were removed from the recommendation dataset, i.e., the MSE was calculated using the 69% of the cases that had recommendations.

In addition to the MSE metric, a check was made on recommendations that had a dimensional difference between y_true and y_rec greater than 0.5mm. With an error less than or equal to 0.5mm it is still possible to do rework on the rotor helicoid, this rework consists of adding a layer of hard-chrome over the helicoid or removing it by sanding. Recommendations with differentials greater than 0.5mm affect the profile of the rotor helicoid, which in turn affects the sealing between the cavities. In this context 6% of the cases tested showed a dimensional difference between y_true and y_rec greater than 0.5mm and 94% less than 0.5mm.

Lastly, visual sample checks were performed by grouping the test results by pump model, except for pump pressure. Figure 6 shows in graph form 20 samples of different pump models comparing their real dimensions with the recommended dimensions. It is
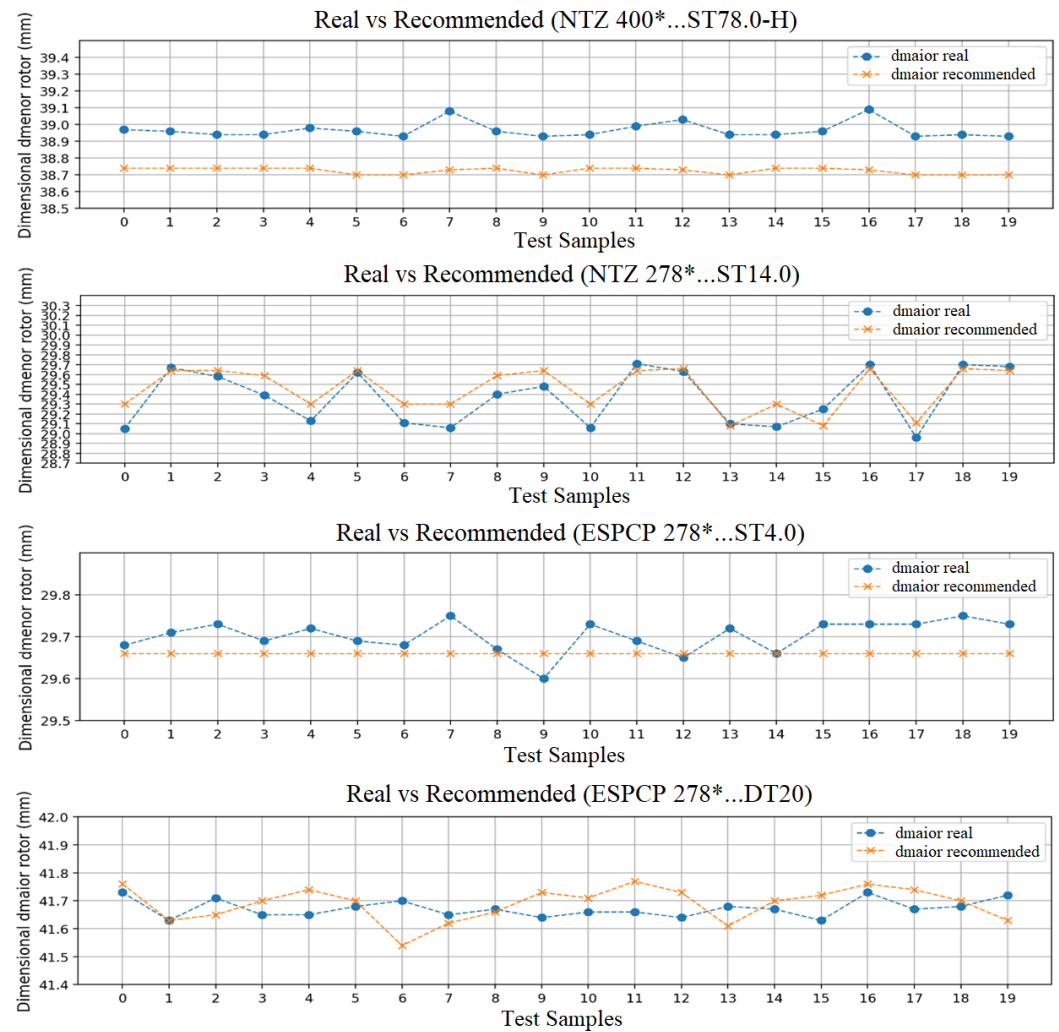
Figure 6. Real vs. recommended dimensional comparison.

possible to see a similarity between the real dimension and the dimension recommended by the recommendation. The dimension of the rotor represented by the y axis shows a decimal variation between the dimensions, in some cases the precision is even lower, in others the recommendation is identical to the real dimension.

Although there is a variation between the real dimension and the recommended dimension, it is worth pointing out that this variation is very small and considered acceptable for this context, since to calculate the dimensions of the rotors the stator measures are used, which can suffer dimensional variations that are reflected in the calculated dimensions of the rotor. Besides this, in the current process there is a cycle time of approximately 62 minutes to perform the Pump Sizing of each Order Acknowledgment. With the implementation of the proposed method, we estimate the reduction of this time, for cases in which there are recommendations, in about 50% for each Order Acknowledgment for which the Pump Sizing is done.

4. Conclusions

This work presented a method for building an interference recommender, helping users in decision making and accelerating steps performed during the Pump Sizing process. Besides the interference recommended, it was possible to diagnose the data used by the recommender, so that an evaluation can be done by experts to try to explain the recommendation, even in cases where the recommendation is not aligned with the user's definition. Thus, with the help of the recommender, besides delivering a recommendation,

the amount of data analyzed by it is much larger if compared to the amount of data that is manually analyzed by the user in the current process.

During the data selection and cleaning stage, several problems related to data quality were identified, due to some legacy systems, which have not been updated during the change of processes over the years, and the use of Excel tables where, both scenarios, give users the freedom to register information without any kind of standardization. In this context, it was decided to eliminate the doubtful records or those with empty fields, impoverishing the database used in this work.

The use of complex networks proved to be very assertive; the construction of a graph represented very well the current analysis model where, during the Pump Sizing process, previous Order Confirmations are used as a reference. In this scenario, Order Acknowledgments were represented by vertices and edges indicate references to other Order Acknowledgments. This allows you to identify the connected components that helped you find similar Order Acknowledgments among the data. In addition to the connected components, the Betweenness Centrality metric can be used to measure the importance of each vertex in the graph, using this measure to recommend the most important Order Acknowledgments to the user and that consequently were the most used in past definitions.

With this, in the tests performed, the method proved to be very efficient. The recommendation index close to 70% already represents a considerable reduction of user time when performing Pump Sizing, even if the result does not agree with the user's opinion, he/she can use the data selected by the recommendation to evaluate the results. In addition, the MSE metric reached a value of 0.28 validating the closeness of the recommended dimensional to the real dimensional measured on the rotor. Finally, a sample comparison of the recommended and real dimensional values showed acceptable recommendations to start testing in a production environment with experts following up to perform a final evaluation. Despite achieving good results in a test environment, it is worth mentioning that it is possible to achieve better recommendation levels by enriching the database, including new variables for verification, implementing new pump model similarity algorithms, performing a seasonal decomposition on the data, among others.

References

1. Assmann, B.W. Estudo de estratégias de otimização para poços de petróleo com elevação por bombeio de cavidades progressivas. Phd thesis, Universidade Federal do Rio Grande do Norte, Natal, Brazil, 2008.
2. Ewert, P.; Kowalski, C.T.; Jaworski, M. Comparison of the Effectiveness of Selected Vibration Signal Analysis Methods in the Rotor Unbalance Detection of PMSM Drive System. *Electronics* **2022**, *11*, 1748. doi:10.3390/electronics11111748.
3. Stefenon, S.F.; Nied, A. FEM Applied to Evaluation of the Influence of Electric Field on Design of the Stator Slots in PMSM. *IEEE Latin America Transactions* **2019**, *17*, 590–596. doi:10.1109/TLA.2019.8891883.
4. Stefenon, S.F.; Seman, L.O.; Schutel Furtado Neto, C.; Nied, A.; Seganfredo, D.M.; Garcia da Luz, F.; Sabino, P.H.; Torreblanca González, J.; Quietinho Leithardt, V.R. Electric Field Evaluation Using the Finite Element Method and Proxy Models for the Design of Stator Slots in a Permanent Magnet Synchronous Motor. *Electronics* **2020**, *9*, 1975. doi:10.3390/electronics9111975.
5. Stefenon, S.F.; Seman, L.O.; Pavan, B.A.; Ovejero, R.G.; Leithardt, V.R.Q. Optimal design of electrical power distribution grid spacers using finite element method. *IET Generation, Transmission & Distribution* **2022**, *16*, 1865–1876. doi:10.1049/gtd2.12425.

6. Stefenon, S.F.; Furtado Neto, C.S.; Coelho, T.S.; Nied, A.; Yamaguchi, C.K.; Yow, K.C. Particle swarm optimization for design of insulators of distribution power system based on finite element method. *Electrical Engineering* **2022**, *104*, 615–622. doi:10.1007/s00202-021-01332-3.

7. Stefenon, S.F.; Americo, J.P.; Meyer, L.H.; Grebogi, R.B.; Nied, A. Analysis of the Electric Field in Porcelain Pin-Type Insulators via Finite Elements Software. *IEEE Latin America Transactions* **2018**, *16*, 2505–2512. doi:10.1109/TLA.2018.8795129.

8. Itajiba, J.A.; Varnier, C.A.C.; Cabral, S.H.L.; Stefenon, S.F.; Leithardt, V.R.Q.; Ovejero, R.G.; Nied, A.; Yow, K.C. Experimental Comparison of Preferential vs. Common Delta Connections for the Star-Delta Starting of Induction Motors. *Energies* **2021**, *14*, 1318. doi:10.3390/en14051318.

9. Sopelsa Neto, N.F.; Stefenon, S.F.; Meyer, L.H.; Ovejero, R.G.; Leithardt, V.R.Q. Fault Prediction Based on Leakage Current in Contaminated Insulators Using Enhanced Time Series Forecasting Models. *Sensors* **2022**, *22*, 6121. doi:10.3390/s22166121.

10. Medeiros, A.; Sartori, A.; Stefenon, S.F.; Meyer, L.H.; Nied, A. Comparison of artificial intelligence techniques to failure prediction in contaminated insulators based on leakage current. *Journal of Intelligent & Fuzzy Systems* **2022**, *42*, 3285–3298. doi:10.3233/JIFS-211126.

11. Stefenon, S.F.; Freire, R.Z.; Coelho, L.S.; Meyer, L.H.; Grebogi, R.B.; Buratto, W.G.; Nied, A. Electrical Insulator Fault Forecasting Based on a Wavelet Neuro-Fuzzy System. *Energies* **2020**, *13*, 484. doi:10.3390/en13020484.

12. Stefenon, S.F.; Singh, G.; Yow, K.C.; Cimatti, A. Semi-ProtoPNet Deep Neural Network for the Classification of Defective Power Grid Distribution Structures. *Sensors* **2022**, *22*, 4859. doi:10.3390/s22134859.

13. Stefenon, S.F.; Corso, M.P.; Nied, A.; Perez, F.L.; Yow, K.C.; Gonzalez, G.V.; Leithardt, V.R.Q. Classification of insulators using neural network based on computer vision. *IET Generation, Transmission & Distribution* **2021**, *16*, 1096–1107. doi:10.1049/gtd2.12353.

14. Corso, M.P.; Perez, F.L.; Stefenon, S.F.; Yow, K.C.; Ovejero, R.G.; Leithardt, V.R.Q. Classification of Contaminated Insulators Using k-Nearest Neighbors Based on Computer Vision. *Computers* **2021**, *10*, 112. doi:10.3390/computers10090112.

15. Stefenon, S.F.; Seman, L.O.; Sopelsa Neto, N.F.; Meyer, L.H.; Nied, A.; Yow, K.C. Echo state network applied for classification of medium voltage insulators. *International Journal of Electrical Power & Energy Systems* **2022**, *134*, 107336. doi:10.1016/j.ijepes.2021.107336.

16. Sopelsa Neto, N.F.; Stefenon, S.F.; Meyer, L.H.; Bruns, R.; Nied, A.; Seman, L.O.; Gonzalez, G.V.; Leithardt, V.R.Q.; Yow, K.C. A Study of Multilayer Perceptron Networks Applied to Classification of Ceramic Insulators Using Ultrasound. *Applied Sciences* **2021**, *11*, 1592. doi:10.3390/app11041592.

17. Duarte, L.B. Cálculo do Rendimento Energético Global do Sistema de Bombas de Cavidades Progressivas com Acionamento Hidráulico. PhD thesis, Centro de Educação Superior da Foz do Itajaí, Balneário Camboriú, Brazil, 2017.

18. Petrowiki. PCP sizing practices. http://petrowiki.org/PCP_sizing_practices/, accessed on September 1, 2022.

19. de Oliveira, J.R.; Stefenon, S.F.; Klaar, A.C.R.; Yamaguchi, C.K.; da Silva, M.P.; Salvador Bizotto, B.L.; Silva Ogoshi, R.C.; Gequelin, E.d.F. Enterprise Resource Planning and Customer Relationship Management Through Management of the Supply Chain. *Interciencia* **2018**, *43*, 784–791.

20. Scarselli, F.; Gori, M.; Tsoi, A.C.; Hagenbuchner, M.; Monfardini, G. The Graph Neural Network Model. *IEEE Transactions on Neural Networks* **2009**, *20*, 61–80. doi:10.1109/TNN.2008.2005605.

21. Fernandes, F.; Stefenon, S.F.; Seman, L.O.; Nied, A.; Ferreira, F.C.S.; Subtil, M.C.M.; Klaar, A.C.R.; Leithardt, V.R.Q. Long short-term memory stacking model to predict the number of cases and deaths caused by COVID-19. *Journal of Intelligent & Fuzzy Systems* **2022**, *6*, 6221–6234. doi:10.3233/JIFS-212788.

22. Vieira, J.C.; Sartori, A.; Stefenon, S.F.; Perez, F.L.; de Jesus, G.S.; Leithardt, V.R.Q. Low-Cost CNN for Automatic Violence Recognition on Embedded System. *IEEE Access* **2022**, *10*, 25190–25202. doi:10.1109/ACCESS.2022.3155123.

23. dos Santos, G.H.; Seman, L.O.; Bezerra, E.A.; Leithardt, V.R.Q.; Mendes, A.S.; Stefenon, S.F. Static Attitude Determination Using Convolutional Neural Networks. *Sensors* **2021**, *21*, 6419. doi:10.3390/s21196419.

24. Stefenon, S.F.; Bruns, R.; Sartori, A.; Meyer, L.H.; Ovejero, R.G.; Leithardt, V.R.Q. Analysis of the Ultrasonic Signal in Polymeric Contaminated Insulators Through Ensemble Learning Methods. *IEEE Access* **2022**, *10*, 33980–33991. doi:10.1109/ACCESS.2022.3161506.

25. Stefenon, S.F.; Ribeiro, M.H.D.M.; Nied, A.; Yow, K.C.; Mariani, V.C.; dos Santos Coelho, L.; Seman, L.O. Time series forecasting using ensemble learning methods for emergency prevention in hydroelectric power plants with dam. *Electric Power Systems Research* **2022**, *202*, 107584. doi:10.1016/j.epsr.2021.107584.

26. Stefenon, S.F.; Ribeiro, M.H.D.M.; Nied, A.; Mariani, V.C.; Coelho, L.S.; Leithardt, V.R.Q.; Silva, L.A.; Seman, L.O. Hybrid Wavelet Stacking Ensemble Model for Insulators Contamination Forecasting. *IEEE Access* **2021**, *9*, 66387–66397. doi:10.1109/ACCESS.2021.3076410.

27. Schmidt, J.; Pettersson, L.; Verdozzi, C.; Botti, S.; Marques, M.A. Crystal graph attention networks for the prediction of stable materials. *Science Advances* **2021**, *7*, eabi7948. doi:10.1126/sciadv.abi7948.

28. Zhang, S.; Tong, H.; Xu, J.; Maciejewski, R. Graph convolutional networks: a comprehensive review. *Computational Social Networks* **2019**, *6*, 1–23. doi:10.1186/s40649-019-0069-y.

29. Zhang, C.; Song, D.; Huang, C.; Swami, A.; Chawla, N.V. Heterogeneous graph neural network. In Proceedings of the Proceedings of the 25th ACM SIGKDD international conference on knowledge discovery & data mining, 2019, pp. 793–803. doi:10.1145/3292500.3330961.

30. Wang, X.; Ji, H.; Shi, C.; Wang, B.; Ye, Y.; Cui, P.; Yu, P.S. Heterogeneous graph attention network. In Proceedings of the The world wide web conference, 2019, pp. 2022–2032. doi:10.1145/3308558.3313562.

31. Stefenon, S.F.; Silva, M.C.; Bertol, D.W.; Meyer, L.H.; Nied, A. Fault diagnosis of insulators from ultrasound detection using neural networks. *Journal of Intelligent & Fuzzy Systems* **2019**, *37*, 6655–6664. doi:10.3233/JIFS-190013.

32. Stefenon, S.F.; Branco, N.W.; Nied, A.; Bertol, D.W.; Finardi, E.C.; Sartori, A.; Meyer, L.H.; Grebogi, R.B. Analysis of training techniques of ANN for classification of insulators in electrical power systems. *IET Generation, Transmission & Distribution* **2020**, *14*, 1591–1597. doi:10.1049/iet-gtd.2019.1579.

33. Stefenon, S.F.; Kasburg, C.; Freire, R.Z.; Silva Ferreira, F.C.; Bertol, D.W.; Nied, A. Photovoltaic power forecasting using wavelet Neuro-Fuzzy for active solar trackers. *Journal of Intelligent & Fuzzy Systems* **2021**, *40*, 1083–1096. doi:10.3233/JIFS-201279.

34. Kasburg, C.; Stefenon, S.F. Deep Learning for Photovoltaic Generation Forecast in Active Solar Trackers. *IEEE Latin America Transactions* **2019**, *17*, 2013–2019. doi:10.1109/TLA.2019.9011546.

35. Stefenon, S.F.; Freire, R.Z.; Meyer, L.H.; Corso, M.P.; Sartori, A.; Nied, A.; Klaar, A.C.R.; Yow, K.C. Fault detection in insulators based on ultrasonic signal processing using a hybrid deep learning technique. *IET Science, Measurement & Technology* **2020**, *14*, 953–961. doi:10.1049/iet-smt.2020.0083.

36. Stefenon, S.F.; Kasburg, C.; Nied, A.; Klaar, A.C.R.; Ferreira, F.C.S.; Branco, N.W. Hybrid deep learning for power generation forecasting in active solar trackers. *IET Generation, Transmission & Distribution* **2020**, *14*, 5667–5674. doi:10.1049/iet-gtd.2020.0814.

37. Leithardt, V.R.Q. Classifying garments from fashion-MNIST dataset through CNNs. *Advances in Science, Technology and Engineering Systems Journal* **2021**, *6*, 989–994.

38. Jiménez Bravo, D.M.; Murciego, A.L.; Crocker, P.; Leithardt, V.R.Q.; de Paz, J.F. Can user data improve Bike Sharing Systems demand forecasting? In Proceedings of the 2021 Telecoms Conference (ConfTELE), 2021, Vol. 1, pp. 1–6. doi:10.1109/ConfTELE50222.2021.9435497.

39. Ribeiro, M.H.D.M.; Stefenon, S.F.; de Lima, J.D.; Nied, A.; Mariani, V.C.; Coelho, L.S. Electricity Price Forecasting Based on Self-Adaptive Decomposition and Heterogeneous Ensemble Learning. *Energies* **2020**, *13*, 5190. doi:10.3390/en13195190.

40. García, R.M.; de la Iglesia, D.H.; de Paz, J.F.; Leithardt, V.R.Q.; Villarrubia, G. Urban Search and Rescue with Anti-pheromone Robot Swarm architecture. In Proceedings of the 2021 Telecoms Conference (ConfTELE), 2021, pp. 1–6. doi:10.1109/ConfTELE50222.2021.9435557.

41. Keiko Yamaguchi, C.; Stefenon, S.F.; Ramos, N.K.; Silva dos Santos, V.; Forbici, F.; Rodrigues Klaar, A.C.; Silva Ferreira, F.C.; Cassol, A.; Marietto, M.L.; Farias Yamaguchi, S.K.; et al. Young People's Perceptions about the Difficulties of Entrepreneurship and Developing Rural Properties in Family Agriculture. *Sustainability* **2020**, *12*, 8783. doi:10.3390/su12218783.

42. da Cruz, F.C.; Stefenon, S.F.; Furtado, R.G.; Rocca, G.A.D.; Ferreira, F.C.S. Financial Feasibility Study for Radio Installation Link on the Mobile Telephone Network. *Revista GEINTEC-Gestão, Inovação e Tecnologias* **2018**, *8*, 4447–4460.

43. Righez, F.O.; Dela Rocca, G.A.; Arruda, P.A.; Stefenon, S.F. Analysis of Technical and Financial Viability of a Fixed Site Internet Broadband. *Revista GEINTEC-Gestão, Inovação e Tecnologias* **2016**, *6*, 3537–3552.

44. Corso, M.P.; Stefenon, S.F.; Couto, V.F.; Cabral, S.H.L.; Nied, A. Evaluation of Methods for Electric Field Calculation in Transmission Lines. *IEEE Latin America Transactions* **2018**, *16*, 2970–2976. doi:10.1109/TLA.2018.8804264.

45. Stefenon, S.F.; Oliveira, J.R.; Coelho, A.S.; Meyer, L.H. Diagnostic of Insulators of Conventional Grid Through Lab-VIEW Analysis of FFT Signal Generated from Ultrasound Detector. *IEEE Latin America Transactions* **2017**, *15*, 884–889. doi:10.1109/TLA.2017.7910202.

46. Muniz, R.N.; Stefenon, S.F.; Buratto, W.G.; Nied, A.; Meyer, L.H.; Finardi, E.C.; Kühl, R.M.; Sá, J.A.S.d.; Rocha, B.R.P.d. Tools for Measuring Energy Sustainability: A Comparative Review. *Energies* **2020**, *13*, 2366. doi:10.3390/en13092366.

47. Matteussi, K.J.; dos Anjos, J.C.S.; Leithardt, V.R.Q.; Geyer, C.F.R. Performance Evaluation Analysis of Spark Streaming Backpressure for Data-Intensive Pipelines. *Sensors* **2022**, *22*. doi:10.3390/s22134756.

48. Cabral, S.H.L.; Bertoli, S.L.; Medeiros, A.; Hillesheim, C.R.; De Souza, C.K.; Stefenon, S.F.; Nied, A.; Leithardt, V.R.Q.; González, G.V. Practical Aspects of the Skin Effect in Low Frequencies in Rectangular Conductors. *IEEE Access* **2021**, *9*, 49424–49433. doi:10.1109/ACCESS.2021.3069821.

49. Stefenon, S.F.; Steinheuser, D.F.; da Silva, M.P.; Silva Ferreira, F.C.; Rodrigues Klaar, A.C.; de Souza, K.E.; Godinho Junior, A.; Vencao, A.T.; Branco, R.; Yamaguchi, C.K. Application of active methodologies in engineering education through the integrative evaluation at the universidade do planalto catarinense, Brazil. *Interciencia* **2019**, *44*, 408–413.

50. Pinto, H.; Américo, J.; Leal, O.; Stefenon, S. Development of Measurement Device and Data Acquisition for Electric Vehicle. *Revista GEINTEC-Gestão, Inovação e Tecnologias* **2021**, *11*, 5809–5822.

51. Leithardt, V.; Santos, D.; Silva, L.; Viel, F.; Zeferino, C.; Silva, J. A Solution for Dynamic Management of User Profiles in IoT Environments. *IEEE Latin America Transactions* **2020**, *18*, 1193–1199. doi:10.1109/TLA.2020.9099759.

52. Viel, F.; Silva, L.A.; Valderi Leithardt, R.Q.; Zeferino, C.A. Internet of Things: Concepts, Architectures and Technologies. In Proceedings of the 2018 13th IEEE International Conference on Industry Applications (INDUSCON), 2018, pp. 909–916. doi:10.1109/INDUSCON.2018.8627298.

53. Mendes, A.S.; Silva, L.A.; Blas, H.S.S.; Jiménez Bravo, D.M.; Leithardt, V.R.O.; González, G.V. WCIoT: A Smart Sensors Orchestration for Public Bathrooms using LoRaWAN. In Proceedings of the 2021 Telecoms Conference (ConfTELE), 2021, pp. 1–5. doi:10.1109/ConfTELE50222.2021.9435574.

54. Stefenon, S.F.; Grebogi, R.B.; Freire, R.Z.; Nied, A.; Meyer, L.H. Optimized Ensemble Extreme Learning Machine for Classification of Electrical Insulators Conditions. *IEEE Transactions on Industrial Electronics* **2020**, *67*, 5170–5178. doi:10.1109/TIE.2019.2926044.
55. Stefenon, S.F.; Ribeiro, M.H.D.M.; Nied, A.; Mariani, V.C.; Coelho, L.S.; da Rocha, D.F.M.; Grebogi, R.B.; Ruano, A.E.B. Wavelet group method of data handling for fault prediction in electrical power insulators. *International Journal of Electrical Power & Energy Systems* **2020**, *123*, 106269. doi:10.1016/j.ijepes.2020.106269.